Photochemical and Photophysical Properties of Rhodium(III) Complexes. Aquation and Luminescence Resulting from Ligand Field Excitation of Pentaamminerhodium(III) Complexes, $Rh(NH_3)_5L^{3+}$

John D. Petersen,[1] Richard J. Watts, and Peter C. Ford*[2]

Contribution from the Department of Chemistry, University of California, Santa Barbara, California 93106. *Received September 12, 1975*

Abstract: Reported are the photoaquation quantum yields (aqueous solution, 298 K) and luminescence spectra and lifetimes (77 K) for a series of rhodium(III) complexes, $Rh(NH_3)_5L^{3+}$ (L = acetonitrile, benzonitrile, pyridine, 3-chloropyridine, 4-methylpyridine). Also reported are the syntheses of the various pyridine complexes. For these complexes irradiation of the lowest ligand field absorption band with 313-nm light leads almost exclusively to aquation of the unique ligand (e.g., when L is acetonitrile, $\Phi_L = 0.47 \pm 0.04$ and $\Phi_{NH_3} < 2 \times 10^{-3}$) despite the proximity of these ligands to NH_3 on a Rh(III) spectrochemical series. The λ_{max} of the lowest energy ligand field band in aqueous solution is approximately the same for the various $Rh(NH_3)_5L^{3+}$; however, the emission band energies are a function of L in a manner which can be rationalized in terms of the relative importance of σ- and π-bonding in the ground and excited states. In general, those $Rh(NH_3)_5L^{3+}$ complexes, which are the more photoreactive in aqueous solution, have the lower energy emission maxima and shorter measured emission lifetimes in low temperature $MeOH/H_2O$ glasses. Thus it is concluded that there are close connections between the structural factors which affect the photochemical and photophysical radiationless decay processes in these complexes. The perdeuterioammine complexes $Rh(ND_3)_5L^{3+}$ (L = py or py-d_5) were also studied, and it is shown that the deuterium isotope effect is to increase the emission lifetime at 77 K and the quantum yield for pyridine photoaquation 298 K. This effect is interpreted in terms of a weak coupling mechanism contributing to the nonradiative deactivation pathways under both sets of conditions.

The photochemical properties of low spin, hexacoordinate nd^6 transition metal complexes have been the subject of extensive research in recent years.[3,4] Of the group 8 metals, the rhodium(III) ammine complexes provide an excellent opportunity for mechanistic evaluation of ligand field (LF) excited state reactivity with minimal complications from excited state manifolds of a different orbital parentage. Thermally stable Rh(III) pentaamine complexes, $Rh^{III}(NH_3)_5L$, can be studied for ligands (L) of the full spectrochemical series, and the relative difficulty of forming Rh(II) gives redox reactions a much less important role in their photochemistry. The Rh(III) LF states are substantially more reactive than the corresponding states of widely studied Co(III) homologues.[5,6] Another important difference between the Co(III) and Rh(III) amines is that the rhodium(III) amine complexes photoluminesce in low temperature glasses, and lifetimes and emission spectra of the lowest energy LF states can be determined.[7-9] This property provides a powerful tool for characterizing the lowest energy LF states.

Previous quantitative photochemical studies of Rh(III) have included the pentaammine complexes of the halide ions,[6,10] azide,[11] and water,[12] the hexaammine complex,[13] and several tetramine complexes.[14,15] Reported here are results of an investigation of the photosubstitution pathways resulting from ligand field excitation of a series of $Rh(NH_3)_5L^{3+}$ complexes. Also reported are the low temperature luminescence spectra and emission life times of these species. In each case the ligand L is an uncharged nitrogen base, either an organonitrile or a substituted pyridine, and the apparent ligand field strength, as derived from the energy of the lowest absorption band (^1E, $^1A_2 \leftarrow {}^1A_1$), is approximately the same. However, the emission band energies and photoaquation quantum yields vary significantly over the same selection of ligands. Thus, in these cases, the energies of the Franck-Condon states reached by initial excitation do not provide a reliable guide either to the relative energies of the thermally equilibrated triplet states or to the reactivities of these states.

Experimental Section

Syntheses. The pentaamminerhodium(III) complexes, $[Rh(NH_3)_5L][ClO_4]_3$ (L = CH_3CN,[16] C_6H_5CN,[16] ammonia,[13] pyrazine,[17] or H_2O[12]), were prepared by procedures described elsewhere.

$[Rh(NH_3)_5py][ClO_4]_3$ was prepared by a procedure modified from that used for the organonitrile complexes.[16] A 0.2-g (0.4 mmol) sample of $[Rh(NH_3)_5H_2O][ClO_4]_3$ was placed into a round-bottom flask with 8 ml of dimethylacetamide. The flask was fitted with a condenser topped with a drying tube filled with $CaSO_4$. The flask was heated in an oil bath for 2 h at 100–110°, then the temperature was reduced to 85° and 1 ml of pyridine (Mallinckrodt-AR) was added. After heating at 85° for 5 h more, the product was precipitated by adding 100 ml of isobutyl alcohol to the reaction solution and cooling the resulting suspension in a refrigerator overnight. The white product was collected and recrystallized from warm water. The recrystallized product was collected, washed with ethanol then ether, and dried under vacuum. Yield of $[Rh(NH_3)_5py][ClO_4]_3$ was 0.12 g (54%). The 3-chloropyridine (3-Cl(py)) and 4-methylpyridine (4-Me(py)) complexes were prepared in the same manner with respective yields of 45 and 77% for the perchlorate salts.

Analyses. Due to the explosive nature of the perchlorate salts, the complexes were reprecipitated as the bromide salts by dissolution in a minimum of water and addition of saturated NaBr solution. The infrared spectra of the resulting solids showed no bands assignable to ClO_4^-.

Anal. Calcd for $C_5H_{20}N_6Br_3Rh$ ($[Rh(NH_3)_5py]Br_3$): C, 11.9; H, 4.0; N, 16.6. Found: C, 11.6; H, 4.2; N, 16.8.

Anal. Calcd for $C_5H_{19}N_6Br_3ClRh$ $[Rh(NH_3)_5(3\text{-}Cl(py))]Br_3$: C, 11.1; H, 3.5; N, 15.5. Found: C, 11.2; H, 4.1; N, 14.9.

Anal. Calcd for $C_6H_{22}N_6Br_3Rh$ $[Rh(NH_3)_5(4\text{-}Me(py))]Br_3$: C, 13.8; H, 4.3; N, 16.1. Calcd for $C_6H_{22}N_6Br_3Rh\cdot H_2O$: C, 13.4; H, 4.5; N, 15.6. Found: C, 13.4; H, 4.4; N, 15.1.

$[Rh(ND_3)_5D_2O][ClO_4]_3$ was prepared by a procedure modified from that used for $[Rh(ND_3)_6][ClO_4]_3$.[13] $[Rh(NH_3)_5H_2O][ClO_4]_3$ (0.58 g, 1.15 mmol) was dissolved in 15 ml of D_2O and converted to the hydroxo complex by the addition of 6 drops of 0.1 N NaOD. The solution was refluxed for 5 h. Three drops of 70% $DClO_4$ in D_2O (Alfa Inorganics) then were added to regenerate the aquo species, and this product was precipitated by the addition of saturated $NaClO_4$ (in D_2O) solution. The mixture was cooled and solid $[Rh(ND_3)_5D_2O][ClO_4]_3$ collected. This procedure was repeated until deuterium substitution (as evaluated by ir) was complete. Yield 0.41 g (71%).

$[Rh(NH_3)_5(py\text{-}d_5)][ClO_4]_3$, $[Rh(ND_3)_5py][ClO_4]_3$, and $[Rh(ND_3)_5(py\text{-}d_5)][ClO_4]_3$ were synthesized by the procedure outlined above. Complexes with deuterated ammines, $Rh(ND_3)_5py^{3+}$ and $Rh(ND_3)_5(py\text{-}d_5)^{3+}$, were prepared from $Rh(ND_3)_5D_2O^{3+}$ and the corresponding pyridine (py and py-d_5, respectively). They were

Table I. Absorption Spectra of Rhodium(III) Amine Complexes in Aqueous Solution[a]

Complex ion	λ_{max} (nm)	ϵ_{max} (M^{-1} cm^{-1})	Assignment
$Rh(NH_3)_6^{3+}$ [b]	305	134	LF
	255	101	LF
$Rh(NH_3)_5(4\text{-}Me(py))^{3+}$ [c]	302	170	LF
	256	2.50×10^3	IL
$Rh(NH_3)_5py^{3+}$ [c]	302	160	LF
	259	2.7×10^3	IL
$Rh(NH_3)_5(3\text{-}Cl\text{-}(py))^{3+}$ [c]	302	170	LF
	272	2.93×10^3	IL
$Rh(NH_3)_5acn^{3+}$ [d]	301	158	LF
	253	126	LF
$Rh(NH_3)_5bzn^{3+}$ [d]	300	339	LF, IL
	282	1.29×10^3	IL
	275	1.55×10^3	IL
	268	1.48×10^3	IL
	245	1.5×10^4	IL
	234	2.04×10^4	IL
$Rh(NH_3)_5\text{-}H_2O^{3+}$ [b]	316	104	LF
	263	89	LF

[a] Dilute solutions of the perchlorate salts at ambient temperature, py = pyridine, acn = acetonitrile, bzn = benzonitrile. [b] Reference 13. [c] This work. [d] Reference 16.

purified by dissolution in D_2O, filtration, and reprecipitation with saturated $NaClO_4$ (in D_2O). Percent deuteration of ammines was estimated from infrared spectra to be >95% D.

$[Rh(NH_3)_5(py\text{-}d_5)][ClO_4]_3$ was prepared by the reaction of $Rh(NH_3)_5H_2O^{3+}$ with pyridine-d_5 (99% D, Stohler Isotope Chemicals) and reprecipitated using H_2O and $NaClO_4$ (in H_2O). The electronic absorption spectra of the variously deuterated pentaammine(pyridine)rhodium(III) complexes were identical within experimental uncertainty: λ_{max} 302 nm (ϵ 160 ± 2 M^{-1} cm^{-1}), 259 ((2.6 ± 0.1) × 10^3).

Photolysis Procedures. Photolyses with 313 and 254-nm light were carried out under thermostated conditions with optical trains and procedures described previously.[12,13] In most cases, quantum yields were obtained from spectral changes (on a Cary 14 spectrophotometer) in the wavelength region of the lowest ligand field absorption band. Spectroscopic quantum yields reported were obtained by plotting interval quantum yields as a function of percent reaction and extrapolating the roughly linear plot to zero percent. Aquation of basic ligands (NH_3 and pyridines) was also examined by measuring pH changes of the photolysis solution during the course of the reaction. Aquation yields of benzonitrile and of pyridine were independently examined by ion exchange analysis of the free ligands released.

Photolyses were carried out in 2-cm quartz cylindrical cells. Sample solutions were prepared gravimetrically such that the optical density at the irradiation wavelength was 0.7–1.7. Each cell was stirred with a 15 × 3 mm, Teflon coated, magnetic stirring bar to maintain solution homogeneity during photolysis. The cells used for photolysis were filled with 6.0 ml of solution. In general, photolysis experiments were run without deoxygenating the solutions; however, representative photolyses carried out under deoxygenated conditions (argon atmosphere) showed no quantum yield differences from those systems saturated with air. Concurrent dark reactions were monitored in each case to evaluate thermal reactions. Under the photolysis conditions, dark reactions were negligible in every case.

Luminescence Procedures. Emission spectra of samples in methanol/water glasses (4/1, v/v) were obtained at 77 K with an apparatus utilizing an Avco C950 pulsed nitrogen laser as the excitation source. The laser produced monochromatic light at 337.1 nm which was focused on the sample cell. The emission was detected using a Ebert-Fastie 0.8-m scanning monochromator (1 mm fixed slits, 1 nm band-pass), followed by a Corning 3-70 glass filter and an EMI 9558 QA phototube. The signal was applied to a Model 164 integrator plug-in unit in a PAR Model 162 boxcar averager. The boxcar averager was triggered by the laser, sampling 0.5–16 μs after the light pulse. The amplified signal was recorded vs. wavelength on a RDK Model B161 strip-chart recorder.

Emission spectra of solid samples were obtained with a continuous source for excitation. The solid salts in a liquid nitrogen quartz Dewar flask (77°) were irradiated at 365 nm with light from a Hanovia 1000-W Hg–Xe lamp which had been passed through a 7-cm solution of $CuSO_4$ (150 g/l.), and a Bausch-Lomb 250-nm monochromator (grating blazed at 300 nm, 5 nm band-pass). The light beam from the monochromator was passed through a PAR Model 191 variable speed chopper. A Corning 7-60 filter followed the chopper to prevent passage of incident irradiation in the same wavelength region as the emission. A Perkin-Elmer Model 98 scanning monochromator was placed at a right angle to the incident light in order to collect light emitted from the sample. An RCA 7102 phototube (cooled with dry ice to minimize the dark current) was used to detect the emission. The signal was applied to the input of a PAR Model 124 lock-in amplifier, and graphically displayed on a RDK Model B161 strip-chart recorder.

The spectral responses of both instruments were calibrated with a NBS L-101 standard lamp to correct for variations with wavelength. All spectra reported have been corrected for spectral response using a computational technique. The corrected spectra obtained from the two apparatus were identical (within experimental uncertainty) for samples of the same complexes in identical media.

The apparatus for the lifetime measurements of solid and glass samples used Avco C950 pulsed nitrogen laser as the excitation source. The 337.1-nm light was passed through a collimation lens, a $CuSO_4$(aq) filter, or a 7-60 Corning glass filter prior to entering the sample holder. An RCA 56TVP phototube, cooled with dry ice, or an EMI 9558 QA phototube, preceded by Corning red glass filters to remove reflected light, was placed at a right angle to the incident light to detect the emission. The signal from the phototube was displayed on a Tektronix Type 549 storage oscilloscope as an intensity vs. time decay curve. A Tektronix Type 184 time mark generator was used to superimpose time marks on the oscilloscope screen to be photographed with the emission and baseline traces.

Results

(1) Absorption Spectra. The electronic spectra absorption maxima of $Rh(NH_3)_5L^{3+}$ complexes important to the photochemical studies here are listed in Table I. Notably, the various complexes having an uncharged nitrogen base as L display longest wavelength absorptions of virtually identical energies and similar intensities despite the differences in the hybridization of the donor nitrogen atoms. This band corresponds to the lowest energy, spin allowed ligand field band of the hexaammine ($^1T_1 \leftarrow {}^1A_1$). Under C_{4v} microsymmetry, the $^1T_1$ LF excited state is split into $^1A_2$ and $^1E^a$; however, for the present cases there is no observable splitting of the $^1E^a$, $^1A_2 \leftarrow {}^1A_1$ absorption. For the substituted pyridine and benzonitrile (bzn) complexes, higher energy LF transitions are obscured by internal ligand (IL) $\pi\pi^*$ transitions. For the aquo and acetonitrile (acn) complexes a second low intensity LF band ($^1E^b$, $^1B_2 \leftarrow {}^1A_1$, corresponding to the $^1T_2 \leftarrow {}^1A_1$ band of the hexaammine) is observed in the absence of IL transitions. Figures 1 and 2 display the spectra of the pyridine and acetonitrile complexes.

(2) Photochemical Studies in Fluid Solution. $Rh(NH_3)_5acn^{3+}$. Photolysis at 313 nm in aqueous solution (pH 2–4, 25°) gave aquation of acetonitrile (eq 1) as the virtually exclusive reaction.

$$Rh(NH_3)_5CH_3CN^{3+} + H_2O \xrightarrow[313\text{ nm}]{h\nu} Rh(NH_3)_5H_2O^{3+} + CH_3CN \quad (1)$$

This wavelength corresponds to the lower energy LF band (Figure 2) and measured quantum yields Φ_L are large (0.47 ± 0.04 mol/einstein, Table II). Solution pH changes do not exceed the experimental uncertainty of the pH meter (±0.01), thus giving an upper limit for Φ_{NH_3} ($\leq 2 \times 10^{-3}$). Long term photolyses of aqueous $Rh(NH_3)_5acn^{3+}$ result in solutions displaying the spectra of aqueous $Rh(NH_3)_5H_2O^{3+}$. For example, irradiation of a 6.0 ml solution of $Rh(NH_3)_5acn^{3+}$ (7.0×10^{-3} M) for ~7 h (313-nm light, $I_0 = 2.8 \times 10^{-6}$ einstein/(l. s)) resulted in a solution with absorption maxima at 314 and

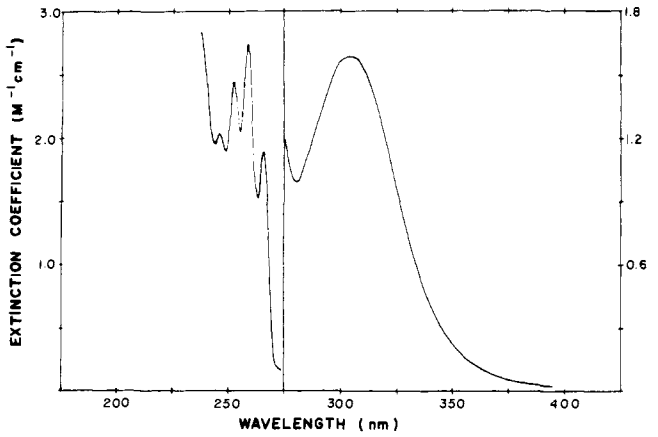

Figure 1. Spectrum of $[Rh(NH_3)_5py][ClO_4]_3$ in dilute aqueous solution. (scale to left is $\times 10^3$, scale to right is $\times 10^2$).

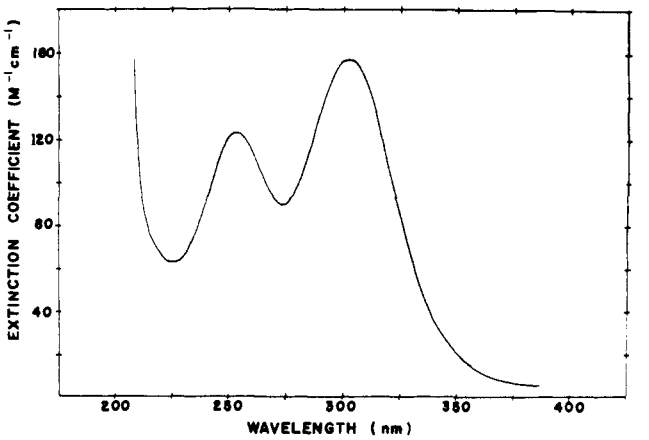

Figure 2. Spectrum of $[Rh(NH_3)_5CH_3CN][ClO_4]_3$ in dilute aqueous solution.

262 nm and calculated molar extinction coefficients of 105 and 95 M^{-1} cm^{-1}, respectively. In comparison $Rh(NH_3)_5H_2O^{3+}$ has band maxima at 316 and 262 nm with ϵ values of 104 and 89 M^{-1} cm^{-1}, respectively. Previously we demonstrated[12] that direct photolysis of $Rh(NH_3)_5H_2O^{3+}$ itself leads to spectrally unobservable H_2O exchange with solvent as the nearly exclusive photoreaction under these conditions. The 313-nm photolysis at 55° gave a modestly higher quantum yield for acetonitrile photoaquation (0.62). The quantum yield differences for these two temperatures give a calculated apparent activation energy (E_a) of 1.8 ± 0.5 kcal/mol.

Irradiation at 254 nm corresponds to excitation of the $^1E^b$, $^1B_2 \leftarrow {}^1A_1$ transition of the acetonitrile complex. Photolysis at this wavelength leads to reactions and quantum yields analogous to those observed with 313 nm irradiation (Table II). The higher upper limits for Φ_{NH_3} in this case are largely due to greater experimental uncertainties derived from lower light intensities at 254 nm.

$Rh(NH_3)_5bzn^{3+}$. The lowest ligand field band maximum for this ion is a shoulder (300 nm) on a more intense IL band. The relatively large excitation coefficient at 300 nm (Table I) suggests that irradiation at 313 nm may involve population of both LF and IL excited states. The 313-nm photolysis of aqueous $Rh(NH_3)_5bzn^{3+}$ leads almost exclusively to aquation of benzonitrile in analogy to eq 1 (Table I). A modest increase in Φ_L was noted for the perdeuterioammine complex in acidic H_2O.

Photolysis at 254 nm clearly involves excitation of internal ligand transitions of very high extinction coefficients. However, irradiation of aqueous $Rh(NH_3)_5bzn^{3+}$ leads to spectral changes analogous to those observed for 313-nm excitation and no change in the solution pH. The conclusion that absorption changes correspond to photoaquation of benzonitrile was confirmed by quantitative chromatographic isolation of the free benzonitrile released.

Pyridine Complexes. The 313-nm photolysis of aqueous $Rh(NH_3)_5py^{3+}$ is accompanied by spectral changes which can be accounted for by the exclusive aquation of coordinated pyridine in acidic solution (eq. 2).

$$Rh(NH_3)_5py^{3+} + H_2O + H^+ \xrightarrow{h\nu} Rh(NH_3)_5H_2O^{3+} + pyH^+ \quad (2)$$

These spectral changes include a shift of the lower energy LF band to a wavelength and intensity corresponding to that of $Rh(NH_3)_5H_2O^{3+}$ plus absorbance increases in the uv region owing to the greater intensities of the π-π^* transition of protonated vs. coordinated pyridine. In addition, ion exchange analysis of reaction solutions gave quantum yields for pyridine release comparable to those obtained by spectral techniques. Solution pH changes can be attributed entirely to the photoaquation of pyridine; therefore, the upper limits for Φ_{NH_3} represent the combined experimental uncertainties of Φ_{py} (spectral) and pH determinations. The quantum yields for the pyridine, 4-methylpyridine, and 3-chloropyridine complexes are reported in Table III.

Photolysis in 40° solution resulted in larger quantum yields for the pyridine and 4-methylpyridine complex, and differences between 25 and 40° give E_a(app) values of 4.4 ± 1.2 and 3.0 ± 1.0 kcal/mol, respectively. Photolysis of the pyridine complex in several concentrations of dilute $HClO_4$ (0.001-0.2 M) led to no systematic difference in Φ_{py}; thus, Φ_{py} is not a function of pH in the manner shown by isoelectronic ruthenium(II) complexes.[18]

Table II. Photoaquation Quantum Yields for $Rh(NH_3)_5acn^{3+}$ and $Rh(NH_3)_5bzn^{3+}$ [a]

Complex ion	λ_{irr} (nm)	Φ_L [b,c]	Φ_{NH_3} [b]
$Rh(NH_3)_5$-acn^{3+}	313	0.47 ± 0.04 (7)	$<2 \times 10^{-3}$
	254	0.48 ± 0.05 (4)	$<7 \times 10^{-2}$
	313[d]	0.62 (1)	$<10^{-2}$
$Rh(NH_3)_5$-bzn^{3+}	313	0.35 ± 0.03 (9)	$<10^{-3}$
	254	0.29 ± 0.04 (4)	$<10^{-3}$
$Rh(ND_3)_5$-bzn^{3+}	313[e]	0.40 ± 0.01 (2)	$<10^{-2}$

[a] Aqueous perchlorate media (pH 2-4), 25 °C except where noted. [b] Moles/einstein. [c] Mean value and average deviation with number of determinations in parentheses. [d] 55 °C. [e] 23 °C.

Table III. Photoaquation Quantum Yields for Substituted Pyridine Complexes $Rh(NH_3)_5pyX^{3+}$ in Aqueous Solution[a]

Complex ion	T, °C	Φ_L [b,c]	Φ_{NH_3} [b]
$Rh(NH_3)_5py^{3+}$	25	0.137 ± 0.014 (6)	<0.02
	40	0.195 ± 0.01 (2)	<0.01
$Rh(NH_3)_5$(4-Me-(py))$^{3+}$	25	0.091 ± 0.003 (8)	<0.01
	40	0.116 ± 0.009 (4)	<0.01
$Rh(NH_3)_5$(3-Cl-(py))$^{3+}$	25	0.341 ± 0.014 (5)	*d*
$Rh(NH_3)_5py\text{-}d_5^{3+}$	25	0.16 ± 0.01 (2)	<0.01
$Rh(ND_3)_5py^{3+}$	25	0.20 ± 0.01 (4)	<0.01
$Rh(ND_3)_5py\text{-}d_5^{3+}$	25	0.225 ± 0.01 (2)	<0.01

[a] pH 2-3 ($HClO_4$), λ_{irr} 313 nm. [b] Moles/einstein. [c] Mean value and average deviation with number of trials in parentheses. [d] Not determined.

Table IV. Emission Spectra and Measured Lifetimes of $[Rh(NH_3)_5L][ClO_4]_3$ Salts as Solutions in $MeOH/H_2O$ (4/1 v/v) Glasses or as Solid Salts at 77 K

	$MeOH/H_2O$ glass			Solid salt		
Complex ion	$\bar{\nu}_{max}$[a]	$\Delta\bar{\nu}_{1/2}$[b]	τ_m[c]	$\bar{\nu}_{max}$[a]	$\Delta\bar{\nu}_{1/2}$[b]	τ_m[c]
$Rh(NH_3)_6^{3+}$	16.4	3.68	18.7 ± 0.7	17.1	3.8	27.2
$Rh(NH_3)_5(4\text{-Me(py)})^{3+}$	16.3	4.00	18.6 ± 1.3	16.6	3.3	22. ± 6
$Rh(NH_3)_5py^{3+}$	16.3	3.66	17.1 ± 1.9	16.9	3.5	24. ± 5
$Rh(NH_3)_5py\text{-}d_5^{3+}$				16.8	3.6	16. ± 7
$Rh(ND_3)_5py^{3+}$				16.9	3.4	60. ± 15
$Rh(ND_3)_5py\text{-}d_5^{3+}$				16.8	3.4	80. ± 10
$Rh(NH_3)_5(3\text{-Cl(py)})^{3+}$	15.6	3.42	13.6 ± 1.5	16.5	3.5	20. ± 8
$Rh(NH_3)_5pz^{3+}$ [d]				15.4	3.3	6.0
$Rh(NH_3)_5bzn^{3+}$	15.8	4.23	7.6 ± 0.9	17.0	5.6	9.0 ± 0.8
$Rh(NH_3)_5acn^{3+}$	15.2	4.0	5.0 ± 0.6	15.3	3.4	7.1 ± 1.0
$Rh(NH_3)_5H_2O^{3+}$	14.9	3.19	2.7 ± 0.5	15.0	3.3	3.4

[a] Energy of emission intensity maximum (corrected) in kK (10^3 cm^{-1}). [b] Bandwidth at one-half maximum intensity in kK. [c] Measured lifetime in μs. [d] pz = pyrazine.

Irradiation of the py and 3-Cl(py) complexes at 254 nm (IL bands) leads to degradation of the pyridine moiety and photoaquation of the complex. Quantum yields were not determined. Although the pyridine decomposition may involve coordinated pyridine, it is equally likely that this process is a secondary photolysis of pyridine released by primary photoaquation of the complex.[19]

Quantum yields for the variously deuterated pentaammine pyridine complexes increase in an apparently systematic fashion as the extent of deuteration is increased. Perdeuteration of the ammonias increases Φ_{py} by approximately 40–50% while perdeuteration of pyridine leads to ~15% increases in Φ_{py}. The latter values, however, lie within the experimental uncertainty of these measurements. Photolysis of the variously deuterated complexes in acidic D_2O solution led to quantum yields identical with those measured in H_2O.

(3) Luminescence Data at 77 K. The luminescence spectra were measured both for solutions in methanol/water glasses (4/1 v/v) and for solid perchlorate salts, $[Rh(NH_3)_5L][ClO_4]_3$. Each compound displayed broad Gaussian emission bands analogous to those previously assigned as LF emissions.[7] The corrected ν_{max} values observed and the bandwidths at half height $\Delta\nu_{1/2}$ are listed in Table IV. Also listed are the measured lifetimes τ_m at 77 K. In general the luminescence behaviors of the solid salts differ systematically from those of the solutions in methanol/water glasses displaying somewhat higher energy emission maxima and somewhat longer lifetimes. The lifetime and ν_{max} values follow the same approximate relative order in both media.

As noted previously,[8] perdeuteration of the coordinated ammines leads to a significantly longer lifetime. $[Rh(ND_3)_5D_2O][ClO_4]_3$ dissolved in a $MeOH/D_2O$ (4/1, v/v) glass displayed a lifetime of 47. ± 10 μs, more than an order of magnitude longer than the fully protonated case. Under these conditions the coordinated water is no doubt substantially protonated, thus the τ_m reported is at best a lower limit for that of the fully deuterated case. Perdeuteration of the ammonias or the pyridine of the pentaammine (pyridine) complex has no effect on the luminescence energy or bandwidth for the emission spectra of the solid perchlorate salts. The perdeuterioammine complexes did have longer measured lifetimes than the perprotio analogues. These τ_m values have large uncertainties as the result of some nonexponentiality for the decay curves due no doubt to the presence of some partially protonated species. Although the perdeuterioammine complexes clearly have longer lifetimes, realistic evaluation would suggest that the reported τ_m values for these complexes should be considered lower limits.

Discussion

The ions $Rh(NH_3)_6^{3+}$ and $Rh(NH_3)_5acn^{3+}$ illustrate the range in the photoproperties reported here. The absorption spectra of the two are qualitatively indistinguishable, the former with LF λ_{max} at 305 and 255 nm, the latter with bands at 301 and 253 nm. The strong field position of acetonitrile in an adsorption spectrochemical series for rhodium(III) ammines is perhaps surprising; yet, this behavior extends to other complexes including those of pentacyanorhodate(III)[20] and pentaamminecobalt(III).[21] Nonetheless, in the emission spectra, the ν_{max}(em) of $Rh(NH_3)_5acn^{3+}$ is significantly below that of $Rh(NH_3)_6^{3+}$. In addition, the photolabilization quantum yields differ by a factor of six. Clearly, features other than the relative energies of the Franck–Condon states reached by initial excitation must be evaluated in interpreting the photochemical and photophysical properties of these complexes.

Previous studies[6] established that the Rh(III) halopentaammines, $Rh(NH_3)_5X^{2+}$, quench triplet biacetyl (but not singlet biacetyl) to give limiting quantum yields equivalent to those observed with direct excitation and concluded that intersystem crossing to the lowest energy LF triplet states[22] occurs with unitary efficiency, perhaps as a result of the large rhodium spin–orbit coupling constant. Sensitization by the triplet donor, pyrazine, has also been noted for $Rh(NH_3)_6^{3+}$ in aqueous solution.[13] In addition the photoquation quantum yields for $Rh(NH_3)_6^{3+}$ and $Rh(NH_3)_5acn^{3+}$ are each independent of whether the lower or higher energy LF absorption band is irradiated, thus implying that initial excitation is followed by interconversion to a common state, presumably the triplet LF state from which emission occurs at reduced temperature.[7,8]

Table V summarizes the photoaquation yields for the $Rh(NH_3)_5L^{3+}$ complexes having uncharged nitrogen bases as the unique ligand. Notably, the Φ_L values follow an order approximately inverse to that of the Bronsted basicities and when $L \neq NH_3$, Φ_L is much larger than Φ_{NH_3} from the same complex, thus demonstrating a definite preference for aquation of the weaker base from a specific complex. Also while the three pyridine complexes listed have identical λ_{max} values for the lowest energy LF band, they range in photoactivity by a factor of about four in a manner reflecting the difference in ligand basicities.

The emission spectra in low temperature glass (Table V) are also responsive to the nature of L with the weaker bases showing the lower energy emission maxima. A similar pattern is observed for the calculated energy E_T of the emitting state

Table V. Photoaquation Quantum Yields and Photoemission Data for $Rh(NH_3)_5L^{3+}$ Complexes in Solution[a]

L	λ_{max}[b] (nm)	$pK_a(L)$[c]	Φ_L[d] (mol/einstein)	$\nu_{max}(em)$[e] (kK)	E_T[f] (kK)	τ_m[e] (μs)
NH_3	305	9.3	0.075[g]	16.4	21.2	18.7
4-Me(py)	302	6.0	0.091	16.3	21.4	18.6
py	302	5.3	0.14	16.3	21.0	17.1
3-Cl(py)	302	2.8	0.34	15.6	20.0	13.6
bzn	300	~−10	0.35	15.8	21.2	7.6
acn	301	~−10	0.47	15.2	20.3	5.0
H_2O	316		0.43[h]	14.9	19.0	2.7

[a] Perchlorate salts. [b] Lowest energy LF absorption band ($^1T_1 \leftarrow {}^1A$ or $^1E^a$, $^1A_2 \leftarrow {}^1A_1$). [c] pK_a of free ligand in aqueous solution, ref 25. [d] For 313-nm excitation at 298 K in dilute aqueous solution. [e] At 77 K in $MeOH/H_2O$ (4/1, v/v) glass. [f] Calculated energy of the lowest triplet state, see text. [g] Reference 13. [h] Reference 12.

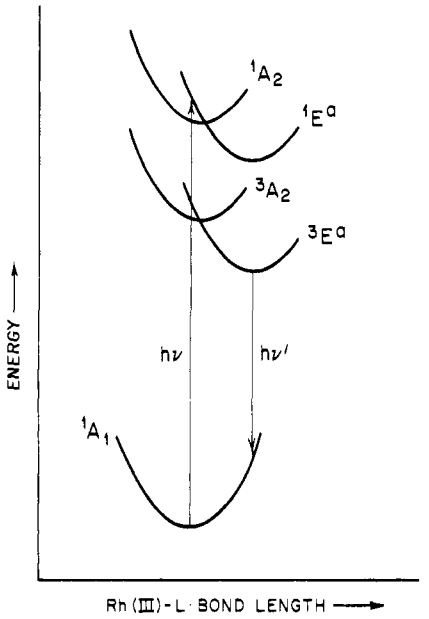

Figure 3. Proposed splitting of A_2, E^a states as a function of distortion along Rh(III)-L bond. $h\nu$ represents the energy of the ligand field absorption maximum in H_2O solution, while $h\nu'$ represents the energy of the emission maximum in $MeOH/H_2O$ glass.

(i.e., the energy of the 0-0 transition from the LF triplet to the ground state). Calculation of this quantity is based on the proposal that the 0-0 energy corresponds roughly to the energy at which the LF emission band is 1% of its maximum intensity on the high energy side of the band.[23] Since emitting contaminants could seriously affect direct measurements of this quantity, a Gaussian curve analysis employing ν_{max} and $\Delta\nu_{1/2}$ (the bandwidth at half height) was used. From the equation for the normalized Gaussian curve one can derive the frequency predicted for 1% intensity on the high energy side according to eq 3.

$$\nu_{1\%} = \nu_{max} + 1.29\Delta\nu_{1/2} = E_T(\text{calcd}) \quad (3)$$

The calculated E_T values follow the same general order as the ν_{max} values with one major exception, the benzonitrile complex. The larger bandwidth for $Rh(NH_3)_5bzn^{3+}$ gives an E_T value comparable to that of $Rh(NH_3)_6^{3+}$. Whether this value represents a physically significant difference between the benzonitrile and acetonitrile complexes or simply the result of the calculation method for E_T is difficult to evaluate.

The relative high energy of the lowest LF absorption bands of $Rh(NH_3)_5L^{3+}$ is perhaps best attributed to a balance of σ and π bonding. Although previous NMR studies[24] with the Rh(III) nitrile complexes demonstrated that π bonding does not involve extensive delocalization into unsaturated ligands, it is possible that a more localized interaction is sufficient to affect the electronic absorption maxima. In this context the acetonitrile complex (C_{4v} symmetry) would be expected to show the d-orbital splitting pattern shown below.

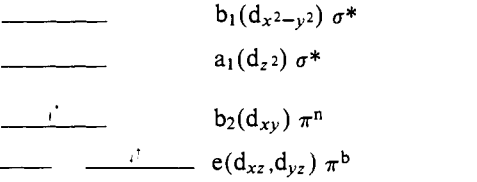

The lower energy one-electron transitions would be $e(d_{xz},d_{yz}) \rightarrow a_1(d_{z^2})$ and $b_2(d_{xy}) \rightarrow b_1(d_{x^2-y^2})$ corresponding to the state transitions $^1E^a \leftarrow {}^1A_1$ and $^1A_2 \leftarrow {}^1A_1$, respectively. In C_{4v} the former would be the more allowed and therefore is probably the principal contributor to the absorption band. π-Bonding should be less significant in the singlet or triplet E^a states. The E^a states are derived from electronic promotion from the π-bonding (d_{xz},d_{yz}) orbitals (thus decreasing π bonding) into the σ-antibonding d_{z^2} orbital. Also in the thermally equilibrated excited ("thexi") state there should be considerable distortion along the unique z axis relative to the ground state. As has been noted previously,[25] d_π-p_π overlap is a more sensitive function to internuclear distance than is d_σ-p_σ or d_σ-sp_σ overlap; therefore, excited state distortion leading to greater metal-ligand distances should decrease the relative contribution of π bonding. Thus, while the Franck-Condon state achieved by vertical excitation to $^1E^a$ may be of comparable or greater energy than that for excitation to $^1A_2$, it is probable that the E^a thexi states lie at significantly lower energy than the A_2 thexi states of analogous mulitiplicity (Figure 3). To a first-order approximation, the $^1A_2 \leftarrow {}^1A_1$ and $^3A_2 \rightarrow {}^1A_1$ transitions of $Rh(NH_3)_5acn^{3+}$ should have energy close to those of the $^1T_1 \leftarrow {}^1A_1$ and $^3T_1 \rightarrow {}^1A_1$ transitions of $Rh(NH_3)_6^{3+}$ Therefore the $Rh(NH_3)_5acn^{3+}$ $^1E^a \leftarrow {}^1A_1$ absorption maximum is understandably close to the lowest energy maximum in the hexaammine spectrum yet the $^3E^a \rightarrow {}^1A_1$ emission band occurs at a significantly lower energy than that for $Rh(NH_3)_6^{3+}$.

It has been argued that, of the three axes described by the ligands of a hexacoordinate complex, d-d excitation will lead to labilization principally along the axis having the weakest average ligand field.[5,26] This is not consistent with the behavior of the $Rh(NH_3)_5L^{3+}$ complexes, *if* the absorption spectra are taken as a measure of the relative ligand field strengths. We agree that the extent to which the excitation is localized by population of the $d_{z^2}(\sigma^*)$ orbital is an important factor in determining the relative photolability of L. However, the comparative σ-donor ability of L is a better criterion for evaluating the extent of d_{z^2} localization in the thexi state than are absorption spectra data for the $Rh(NH_3)_5L^{3+}$ complexes.

The data in Table V indicate that the complexes displaying the higher energy emission maxima in the $MeOH/H_2O$ glass also have the longer lifetimes in this medium at 77 K. Photochemistry is not observed at 77 K and the lifetime can be represented as

$$\tau_m = (k_n + k_r)^{-1} \quad (4)$$

where k_n is the rate constant for nonradiative deactivation and k_r the rate constant for radiative deactivation under these conditions. Since in each case emission is weak, k_n must be substantially greater than k_r, therefore $\tau_m \simeq (k_n)^{-1}$. In this context, the sevenfold decrease in τ_m in going from $Rh(NH_3)_6^{3+}$ to $Rh(NH_3)_5H_2O^{3+}$ can be attributed to a corresponding sevenfold increase in k_n.

Previous workers have drawn attention to the importance of nonradiative deactivation pathways in the photoreactions[6,10,13] and luminescence properties[8,9] of rhodium(III) hexaammine and various halopentaammine complexes. For large molecules, vibronic coupling between an excited state and the ground state has been analyzed in terms of two limiting models,[27-29] *strong coupling* and *weak coupling*. For limiting weak coupling, it is predicted that k_n will increase exponentially as the difference in energy between the ground and excited states decreases and will be dominated by the highest frequency vibrational modes of the molecule,[27] while in the strong coupling limit, k_n will be relatively insensitive to the highest frequency vibrational modes. Thus it is predicted for metal amine complexes that in the weak coupling limit radiationless transition to the ground state primarily involves activation of the N-H vibrations of the coordinated ammonias[30] but in the strong coupling limit involves major distortion (and activation) of the metal ligand bond framework as well. Chemical reaction, such as the dissociation of a ligand is, in principle, a strong coupling process. The dramatic increases in τ_m when the ammonias of the hexaammine and several pentaammine Rh(III) complexes are perdeuterated[8] provide convincing support for the major and probably dominant role of a weak coupling deactivation mechanism at low temperatures. Similarly, the observation of perdeuteration related increases in photoaquation quantum yields resulting from ligand field excitation in fluid solution may indicate (indirectly) the role of a weak coupling deactivation pathway under these conditions (Table III and ref 13). Also, since the spin-orbit constants for the various L's do not differ substantially, the observation that emission lifetimes (in the $MeOH/H_2O$ glasses) are generally shorter for those complexes with lower energy emission maxima (Table V) is consistent with the proposal of a weak coupling deactivation pathway.

Despite the very significant differences between the experimental conditions of the luminescence and photochemical measurements, there is an empirical relation between these data sets for the $Rh(NH_3)_5L^{3+}$ ions. The complexes having higher Φ_L values in ambient temperature fluid solutions generally are those which display lower energy emission maxima and shorter measured lifetimes in low temperature glasses (Table V). The same pattern is observed for the halopentaammines, $Rh(NH_3)_5X^{2+}$. Although combination of the $Rh(NH_3)_5L^{3+}$ and $Rh(NH_3)_5X^{2+}$ series does not give a coherent single series, this can perhaps be attributed to the different spin-orbit coupling constants of the halide ions.

In the absence of luminescence the photoaquation quantum yield can be described by

$$\Phi_L = \Phi_{IC} \frac{k_p}{k_n' + k_p} \quad (5)$$

where Φ_{IC} is the interconversion efficiency from initially populated states to the reactive states, k_p is the rate of aquation, and k_n' the rate of nonradiative deactivation from the excited states. If, as suggested above, initial excitation is followed by efficient deactivation to the lowest energy triplet from which deactivation and aquation occur, then eq 5 can be rewritten as

$$\Phi_L = \frac{k_p}{k_n' + k_p} \quad (6)$$

One possible connection between the luminescence and photochemical experiments is to consider the respective nonradiative deactivation rate constants k_n (eq 4) and k_n' (eq 6) under the two sets of conditions. For both types of experiment and with nearly every $Rh(NH_3)_5L^{3+}$ complex, nonradiative decay to the initial ground state is the major mode of deactivation of the excited states (i.e., $k_n > k_r$ at 77°, $k_n' > k_p$ at 298°). Given the differences in the conditions of the photochemical and luminescence experiments, the pathways described by k_n and k_n', respectively, may have little similarity. However, the deuterium isotope effects observed under luminescence and photochemical conditions for the hexaammine,[13] pentaamminepyridine (Tables III and IV), and chloropentaammine[6] complexes suggest the common thread of a weak coupling mechanism contribution to both k_n and k_n' for these species. Yet, with the consistent exceptions of the deuterium isotope effects, there is no indication whatsoever that increased photolability results from decreases in nonradiative deactivation rates. This contrasts the prediction[26] that increased localization of excitation in the d_{z^2} orbital of C_{4v} and D_{4h} d^6 metal ion complexes will result in decreasing the nonradiative deactivation rate k_n'. We believe instead that the opposite is suggested, namely the more reactive systems may also have larger k_n' values. It is clear, however, that a realistic evaluation of these proposals must await direct measurement of k_n' values under photochemically relevant conditions.

Given the short lives of the relevant excited states, it is clear that the rate constants k_p represent enormous rate accelerations over ground state processes. For example, the rate constant for exchange of coordinated and solvent water for aqueous $Rh(NH_3)_5H_2O^{3+}$ is 6×10^{-6} s^{-1} (293 K),[12] thus the analogous reaction resulting from ligand field excitation must be at least 10 orders of magnitude faster. With regard to possible photoaquation mechanisms, there are three pathways that might lead to ligand photolabilization. These are either an associative or dissociative substitution of an excited state or interconversion of the excited state to a vibrationally excited, ground electronic state ("hot" ground state) followed by aquation of this species.[31] It is possible that a strongly distorted thexi state having a $(t_{2g})^5(e_g)^1$ electronic configuration would show a rate acceleration of the necessary magnitude over its $(t_{2g})^6$ ground state analogue; however, this argument implies largely dissociative process. The "hot" ground state mechanism is also attractive given the arguments[32] that the lowest excited states of Rh(III) ammines have energies in excess of the $\Delta H^{\ddagger}$ values for the substitution reactions of the ground state analogues.[33] Isoenergetic tunneling from the lowest excited state to the ground state would place the complex on high energy vibrational excited state surfaces of the ground electronic state. Various reaction trajectories along these surfaces in competition with vibrational deactivation to the ground state would determine the relative yields of the possible processes. Nonetheless, we do not believe the current data with Rh(III) ammine complexes distinguish between a dissociative reaction of the excited state and a "hot" ground state mechanism for the photoaquation pathways.

In summary, we wish to emphasize the following: (1) Irradiation of $Rh(NH_3)_5L^{3+}$ ligand field absorption bands in ambient aqueous solution results in photochemical aquation, primarily of the unique ligand L while irradiation at 77 K results in photoluminescence but no photochemistry. (2) Data taken from absorption spectra are inadequate to interpret the

observed trends in the photochemical quantum yields; however, our results do suggest a correlation between σ-donor abilities of the ligands, L, and the photoaquation quantum yields. (3) The luminescence spectra of the complexes are sensitive to the nature of the unique ligand, and a definite correlation between the emission band maximum and the photoaquation quantum yield exists: as the energy of the emission band maximum decreases, the photochemical quantum yield increases. (4) Increases in Φ_L at 298 K are paralleled by increases in the radiationless deactivation rate constants at 77 K as L is varied, thus indicating a close connection between the structural factors which affect photochemical and photophysical radiationless decay processes in these complexes.

Acknowledgments. This work was supported by the National Science Foundation (GP-26199 and GP-36643X). The rhodium used in these studies was provided on loan by Matthey-Bishop, Inc.

References and Notes

(1) (a) Taken from the Ph.D. Dissertation of J.D.P., University of California, Santa Barbara, 1975. (b) Reported in part at the 165th National Meeting of the American Chemical Society, Dallas, Texas, April 1973, INORG 39; and at the 169th National Meeting of the American Chemical Society, Philadelphia, Pa., April 1975, INORG 141.
(2) Camille and Henry Dreyfus Foundation Teacher-Scholar, 1971-1976.
(3) General reviews are: (a) V. Balzani and V. Carassiti, "Photochemistry of Coordination Compounds", Academic Press, London, 1970; (b) P. D. Fleischauer, A. W. Adamson, and G. Satori, *Prog. Inorg. Chem.*, **17**, 1 (1972); (c) A. W. Adamson and P. D. Fleischauer, Ed., "Concepts of Inorganic Photochemistry", Wiley, New York, N.Y., 1975.
(4) P. C. Ford, J. D. Petersen, and R. E. Hintze, *Coord. Chem. Rev.*, **14**, 67 (1974).
(5) R. A. Pribush, C. K. Poon, C. M. Bruce, and A. W. Adamson, *J. Am. Chem. Soc.*, **96**, 3027 (1974).
(6) (a) T. L. Kelly and J. F. Endicott, *J. Phys. Chem.*, **76**, 1937 (1972); (b) L. Moggi, *Gazz. Chim. Ital.*, **97**, 1089 (1967).
(7) T. R. Thomas and G. A. Crosby, *J. Mol. Spectrosc.*, **38**, 118 (1971).
(8) T. R. Thomas, R. J. Watts, and G. A. Crosby, *J. Chem. Phys.*, **59**, 2123 (1973).
(9) J. E. Hillis and M. K. DeArmond, *J. Lumin.*, **4**, 273 (1971).
(10) T. L. Kelly and J. F. Endicott, *J. Am. Chem. Soc.*, **94**, 1797 (1972).
(11) (a) J. L. Reed, H. D. Gafney, and F. Basolo, *J. Am. Chem. Soc.*, **96**, 1363 (1974); (b) G. Ferraudi and J. F. Endicott, *ibid.*, **95**, 2371 (1973).
(12) P. C. Ford and J. D. Petersen, *Inorg. Chem.*, **14**, 1404 (1975).
(13) J. D. Petersen and P. C. Ford, *J. Phys. Chem.*, **78**, 1144 (1974).
(14) C. Kutal and A. W. Adamson, *Inorg. Chem.*, **12**, 1454 (1973).
(15) M. M. Muir and W. L. Huang, *Inorg. Chem.*, **12**, 1831 (1973).
(16) R. D. Foust and P. C. Ford, *Inorg. Chem.*, **11**, 899 (1972).
(17) C. Cruetz and H. Taube, *J. Am. Chem. Soc.*, **95**, 1086 (1973).
(18) D. A. Chalsson, R. E. Hintze, D. H. Stuermer, J. D. Petersen, D. P. McDonald, and P. C. Ford, *J. Am. Chem. Soc.*, **94**, 6665 (1972).
(19) J. Joussot-Dublen and J. Houdard, *Tetrahedron Lett.*, **44**, 4389 (1967).
(20) G. L. Geoffroy, M. S. Wrighton, G. S. Hammond, and H. B. Gray, *Inorg. Chem.*, **13**, 430 (1974).
(21) D. A. Buckingham, F. R. Keene, and A. M. Sargeson, *J. Am. Chem. Soc.*, **95**, 5649 (1973).
(22) Given the magnitude of spin–orbit coupling for rhodium(III), the term "triplet" may have questionable validity. However, the observation of sensitization by triplet donors and energy differences between lower energy absorption bands and the emission bands point to the presence of LF states of a character in most respects analogous to the triplet proposed for compounds of the lighter elements. Therefore with some reservation we will conform to the previous description (see ref 4, 6-8, 13, 20) of such states as "triplets".
(23) D. H. Carstens and G. A. Crosby, *J. Mol. Spectrosc.*, **34**, 113 (1970).
(24) R. D. Foust and P. C. Ford, *J. Am. Chem. Soc.*, **94**, 5686 (1972).
(25) R. J. Allen and P. C. Ford, *Inorg. Chem.*, **11**, 679 (1972).
(26) M. J. Incorvia and J. I. Zink, *Inorg. Chem.*, **13**, 2489 (1974).
(27) R. Englman and J. Jortner, *Mol. Phys.*, **18**, 145 (1970).
(28) W. M. Gelbart, K. F. Freed, and S. A. Rice, *J. Chem. Phys.*, **52**, 2460 (1970).
(29) E. W. Schlag, S. Schneider, and S. F. Fischer, *Annu. Rev. Phys. Chem.*, **22**, 465 (1971).
(30) D. J. Robbins and A. J. Thompson, *Mol. Phys.*, **25**, 1103 (1973).
(31) M. Wrighton, H. B. Gray, and G. S. Hammond, *Mol. Photochem.*, **5**, 165 (1973).
(32) J. F. Endicott, presented at the VIIIth International Conference of Photochemistry, Edmonton, Alberta, Canada, Aug 1975.
(33) F. Monocelli and E. Viel, *Inorg. Chim. Acta*, **1**, 467 (1967).

The Temperature Dependence of the Crystal and Molecular Structure of $\Delta^{2,2'}$-Bi-1,3-dithiole [TTF] 7,7,8,8-Tetracyano-*p*-quinodimethane [TCNQ]

Arthur J. Schultz,[1a] Galen D. Stucky,* [1a] Robert H. Blessing,[1b] and Philip Coppens[1b]

Contribution from the Department of Chemistry and the Materials Research Laboratory, University of Illinois, Urbana, Illinois 61801, and the Department of Chemistry, State University of New York at Buffalo, Buffalo, New York 14214. *Received June 17, 1975*

Abstract: In order to structurally define the 53 K metal-insulator transition observed in the charge transfer salt, $\Delta^{2,2'}$-bi-1,3-dithiole [TTF] 7,7,8,8-tetracyano-*p*-quinodimethane [TCNQ], the structures of (TTF) (TCNQ) were examined at 60, 53, and 45 K by single-crystal x-ray diffraction. Systematic changes in other properties of the crystalline complex do appear to be related to the metal-insulator transition temperature. The minimum interplanar spacings along the homologous chains are found to be 3.408 (2) and 3.090 (1) Å for TTF and TCNQ, respectively.

The metal-insulator transition in the one-dimensional conductor TTF-TCNQ has been a subject of intensive investigation following its initial report.[2] The transition is characterized by a conductivity maximum at ~58 K now believed to be on the order of 10-30 times the room temperature conductivity.[3] It was proposed[2b] that a possible mechanism for this behavior would involve a soft phonon mode producing paraconductivity as a result of a lattice distortion at the transition temperature. This type of lattice distortion associated with the metal to insulator transition in one-dimensional conductors is believed to occur in the Krogmann salts, $[K_2Pt(CN)_4]X_{0.3}\cdot XH_2O$ (X = Cl, Br), where evidence for a soft phonon mode, through the observation of a Kohn anomaly, has been reported.[4,5] However, the Krogmann salts do not exhibit a sharp rise and fall in conductivity, and it is this property in TTF-TCNQ that has generated much interest.

The single-crystal x-ray diffraction structures of TTF-TCNQ previously have been reported for room temperature[6] and 100 K[7] data. In this paper, we present the structural results for data collected at 60 K, where the transition, as defined by the heat capacity data, is beginning; at 53 K, where the maximum peak in the heat capacity curve occurs;[8] and at 45 K, which is well into the insulating state. Simi-